ADVANCED FUNCTIONAL MATERIALS
www.afm-journal.de

An Artificial Peripheral Neural System Based on Highly Stretchable and Integrated Multifunctional Sensors

Xinqin Liao, Weitao Song, Xiangyu Zhang, Haoran Jin, Siyu Liu, Yongtian Wang, Aaron Voon-Yew Thean, and Yuanjin Zheng**

Prostheses and robots have been affecting all aspects of life. Making them conscious and intelligent like humans is appealing and exciting, while there is a huge contrast between progress and strong demand. An alternative strategy is to develop an artificial peripheral neural system with high-performance bionic receptors. Here, a novel functional composite material that can serve as a key ingredient to simultaneously construct different artificial exteroceptive sensors (AE sensors) and artificial proprioceptive sensors (AP sensors) is demonstrated. Both AP sensors and AE sensors demonstrate outstandingly high stretchability; up to 200% stretching strain and possess the superior performance of fast response and high stability. An artificial peripheral neural system integrated with the highly stretchable AP sensor and AE sensor is constructed, which makes a significant breakthrough in the perception foundation of efficient proprioception and exteroception for intelligent prostheses and soft robots. Accurate feedback on the activities of body parts, music control, game manipulation, and wireless typing manifest the enormous superiority of the spatiotemporal resolution function of the artificial peripheral neural system, all of which powerfully contribute to promoting intelligent prostheses and soft robots into sophistication, and are expected to make lives more fascinating.

1. Introduction

Peripheral neural system possesses exteroception and proprioception, which provide the body with necessary sensory information to make decisions when interacting with external objects. Exteroceptor, which is a sensory organ or part of the body, such as the eyes, ears, nose, or skin, can receive stimulation from outside the body. These different stimulations in the external environment, including but not limited to light, sound, gas, and pressure, can be transformed by different exteroceptors into sensory nerve impulses, which are then transferred from afferent pathway to the corresponding sensory center to produce different sensations. Through exteroceptor, the body feels a sense of exteroception and thus, understands the characteristics of external objects.[1–3] Proprioceptor, which is also a receptor in blood vessels, skin, or muscles, etc., supplies information about the movement, position, and state of the body and its parts. The muscular tension and pressure and the degree of joints' bending are transformed by different proprioceptors into nerve impulses. Subsequently, the cerebral cortex can receive the nerve impulses through neural pathways and the spinal cord. In such a way, people generate proprioception that is a perception based on the information from proprioceptors and know where the body and limb positions are in space and what their states are.[4,5] Both exteroceptor and proprioceptor are important and often complementary to each other. For example, for a touch action, the motion of the arm is sensed through proprioceptors. Once the finger touches the target object, exteroceptor will respond. Considerable efforts have been made in developing artificial aid equipment, such as prostheses and robots.[6–15] In order for them to be as conscious and intelligent as humans, it is necessary to develop artificial peripheral neural system, while its progress is still far from enough.

Bionic sensors have recently been finitely researched to mimic exteroceptors or proprioceptors, which possess enormous potentialities for condition monitoring and feedback control.[16–19] Inspired by the distributed sensing mechanism of different mechanoreceptors, a haptic sensor based on a hierarchically distributed microstructure was fabricated and could translate pressure stimulation into electronic signals.[20] To

Dr. X. Liao, Dr. W. Song, Dr. H. Jin, Dr. S. Liu, Prof. Y. Zheng
School of Electrical and Electronic Engineering
Nanyang Technological University
50 Nanyang Avenue, Singapore 639798, Singapore
E-mail: liaoxinqin677@163.com; yjzheng@ntu.edu.sg

Dr. X. Liao
Guangdong Provincial Key Laboratory of Malignant Tumor Epigenetics and Gene Regulation
Medical Research Center
Sun Yat-Sen Memorial Hospital
Sun Yat-Sen University
107 Yanjiang West Road, Guangzhou 510120, China

Dr. X. Zhang, Prof. A. V.-Y. Thean
Department of Electrical and Computer Engineering
National University of Singapore
4 Engineering Drive 3, Singapore 117583, Singapore

Prof. Y. Wang
Beijing Engineering Research Centre of Mixed Reality and Advanced Display
School of Optics and Photonics
Beijing Institute of Technology
5 Zhongguancun South Street, Beijing 100081, China

The ORCID identification number(s) for the author(s) of this article can be found under https://doi.org/10.1002/adfm.202101107.

DOI: 10.1002/adfm.202101107

ADVANCED FUNCTIONAL MATERIALS
www.afm-journal.de

recognize control trajectory, an alternative strategy was to construct a sensor array, where numerous sensing elements were connected together by interlaced wires.[21–24] Via designing surface microstructures, flexible sensors were fabricated and put forward as an alternative solution for microstrain monitoring and healthcare.[25–27] Presently, research on bionic exteroceptors or bionic proprioceptors is carried out separately due to their incompatibility, which restricts integration and coordinated operation of bionic sensing system. Few studies have reported on composite functional materials and highly universal processes that simultaneously realize the construction and functioning of two or more different types of bionic receptors. There is a huge contrast between the current progress and strong demand for developing artificial peripheral neural system. Besides, the targeted artificial peripheral neural system strongly desires high stretchability to allow well-pleasing integration of intelligent prostheses with the human body, and to adapt and monitor large deformation of soft robots.

Here we demonstrate a novel functional composite material that can serve as a key ingredient to for the first time simultaneously construct different artificial exteroceptive sensor (AE sensor) and artificial proprioceptive sensor (AP sensor) for artificial peripheral neural system. The functional composite material, which consists of carbon nanotubes (CNTs), polyester fibers, and rubber fiber, is based on the design method of cross-scale heterogeneous structure. Through ingenious structural designs, the AE sensor and AP sensor feature outstandingly high stretchability that is unprecedented up to 200% stretching strain, laying an important perception foundation for intelligent prostheses and soft robots with great elasticity for future applications. Both AE sensor and AP sensor exhibit the superior performance of fast response and high stability, which ensures efficient and stable operation. Thereinto, a free conductive gate structure is proposed to construct the AE sensor. Based on the proposed structure, the AE sensor characterizes geometrically hierarchical sensing capability that enables to translate different location of external mechanical stimulation into a distinct electronic signal. Importantly, the AE sensor realizes the integrated functions of detecting external stimulation, recognizing stimulation location, and transmitting mechanosensitive signal, and features no energy consumption when no external stimulation occurred. It effectively avoids the use of numerous electronic sensing elements and addresses the challenge of complex manufacturing processes of interlaced wires. Attributed to the superior universality of the design principle, the AE sensor can be designed into multiple types of prototype devices for personalized applications, including music control, game manipulation, and wireless typing. Regarding the AP sensor, it characterizes a high sensitivity and an outstandingly wide sensing range, of which gauge factor (GF) is over 28 times and sensing range is 40 times than that of metal-based sensors, respectively. It provides a powerful platform as a wearable health monitoring device to accurately feedback the activities and states of various body parts, such as finger joint, elbow joint, and knee joint. As a proof-of-concept, we explore the spatiotemporal resolution function of an artificial peripheral neural system integrated with the AE sensor and AP sensor. With the help of algorithmic analysis, the artificial peripheral neural system possesses both efficient exteroception and proprioception, and exhibits a great potential to promote intelligent prostheses and soft robots into being conscious. This work not only brings a novel functional composite material to simultaneously realize the fabrication of two different types of highly stretchable bionic receptors but is also expected to achieve a highly significant scientific and technological breakthrough for the research of artificial peripheral neural system.

2. Results and Discussion

The concept behind the mechanosensational artificial peripheral neural system is shown in **Figure 1**. Biologically, as shown in Figure 1a, a stimulation is translated into receptor potentials by multiple mechanoreceptors, such as Meissner corpuscle, Ruffini corpuscle, Merkel disk, and Pacinian corpuscle. With the help of biological synapse, the receptor potentials trigger the generation of postsynaptic potentials, which are then transmitted to the brain through nerve fibers. Finally, the body will generate a perception that means relating to the way people interpret and understand what they notice or feel. Functionally inspired by the somatosensory signal generation, we demonstrated a mechanosensational artificial peripheral neural system, which consisted of the AE sensor and AP sensor, with the huge potential for person identification, motion recognition, wearable interaction, and artificial intelligence (Figure 1b). In our design, the configurations of the AE sensor and AP sensor were ultrasimple and highly efficient, both of which were fabricated of a stretchable active thread.

The AE sensor adopted a parallel configuration of two stretchable active threads with the free conductive gate structure (Figure 1c). When an external mechanical stimulation was not applied, there is no current in the AE sensor due to the fact that the parallel stretchable active threads were separated. In this case, the AE sensor consumed no energy, which was conducive to long-term functioning. Once the external mechanical stimulation was applied on the AE sensor, the free conductive gate would contact with the parallel stretchable active threads and thus, a current in the AE sensor would occur. This was a mechanosensational signal and its value varied with the location of the external mechanical stimulation. Subsequently, the mechanosensational signal would be transmitted through the AE sensor to a back-end microcontroller unit (MCU) for decision-making. Overall, the AE sensor integrated the all-in-one multifunction of converting, recognizing, and transmitting the mechanosensational signal, and featured no energy consumption when no external stimulation occurred. The functional characteristics enabled the AE sensor to provide the efficient exteroception of intelligent prostheses and soft robots. It should be noted that the realization of the exteroception did not need numerous electronic sensing elements and complex manufacturing process of interlaced wires as common, such that greatly simplified the device's structure and made it highly efficient.

The equivalent circuit of the AE sensor was shown in Figure 1d, where the working mechanism of the AE sensor was explained in the electronic aspect. In the equivalent circuit, two parallel resistance strings, each of which composed of numerous variable resistance units, were equivalent to the parallel stretchable active threads. Since the external free

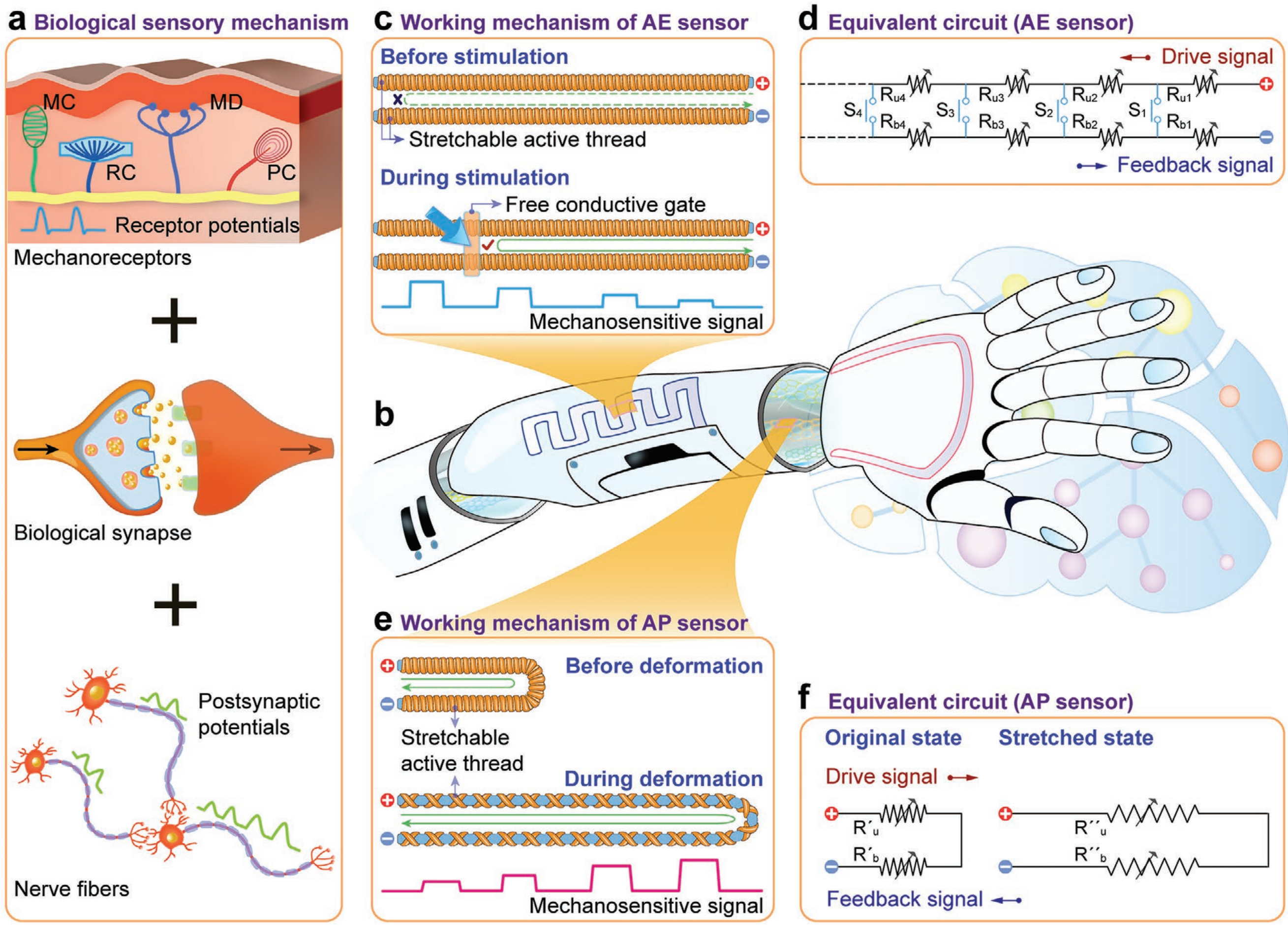

Figure 1. Biological inspiration and design of bionic receptors. a) Illustration of biological mechanoreceptors and the related neural system. b) An intelligent prosthetic limb combined with the AE sensor and AP sensor for interactive applications. c) Design principle and working mechanism of the AE sensor. d) Equivalent circuit for the working principle of the AE sensor. e) Design principle and working mechanism of the AE sensor. f) Equivalent circuit for the working principle of the AE sensor.

conductive gate would contact any location of the stretchable active threads, the current loop would be generated and vary with the involved parts of the stretchable active threads. It could be considered as that there was a plurality of virtual switches between the parallel resistance strings. As an example, when the free conductive gate would contact the S_1 location of the AE sensor due to an external mechanical stimulation, the virtual switch S_1 would close. Followingly, a responding current was generated and transmitted by the AE sensor, where a current loop occurred. The corresponding resistance (R_{total}) of the AE sensor was expressed as: $R_{total} = R_{u1} + R_{b1}$, where the R_{u1} and R_{b1} were the values of the variable resistance units in the parallel resistance strings. Once the location of the external mechanical stimulation changed to S_2 location, the virtual switch S_1 would open while the virtual switch S_2 closed. In this case, the response resistance of the AE sensor was changed and calculated as: $R_{\text{total}} = R_{\text{u1}} + R_{\text{u2}} + R_{\text{b1}} + R_{\text{b2}}$. For other situation that the external mechanical stimulation was applied on S_n location of the AE sensor, the response resistance of the AE sensor could be universally represented by the formula as: $R_{\text{total}} = \sum_{i=1}^{n} (R_{\text{u1}} + R_{\text{u2}} + R_{\text{b1}} + R_{\text{b2}} + \ldots + R_{\text{u}i} + R_{\text{b}i})$. Therefore, the AE sensor could convert the external mechanical stimulation into electrical signal. Different location of the mechanical stimulation would be recognized by the AE sensor due to different value of the response resistance. The generated current went through the AE sensor and was transmitted to the MCU for decision-making.

For the AP sensor, a U-type configuration of the stretchable active thread was adopted (Figure 1e). A drive signal powered by an external voltage of 5 V would directly go through the stretchable active thread to form a feedback signal. When the AP sensor was deformed, the feedback signal would be changed. Once the AP sensor returned to its original state, the feedback signal would turn back. Thus, there was a baseline signal in the AP sensor and a relationship between the feedback signal and deformation. If the baseline signal was defined as the value of the feedback signal when the AP sensor was in the original state, by judging the relationship between the feedback signal and the baseline signal, the deformation would be confirmed. Therefore, the functional characteristics of the AP sensor enabled to realize the proprioception of intelligent prostheses and soft robots. It meant that their joint activity could be detected by the AP sensor, and the amount of deformation would be determined. Based on the information from the AP sensor, intelligent prostheses and soft robots would know where the body or limb position is in space.

To explain the working mechanism of the AP sensor in the electronic aspect, the equivalent circuit of the AP sensor was prepared in Figure 1f. It could be found that two variable resistance units, each of which represented half part of the stretchable active thread, were connected at one end, and side by side in series. The value of each variable resistance unit varied with the deformation. In the original state, the drive signal could directly go through the serial variable resistance units to get a feedback signal. In this case, the corresponding resistance of the AP sensor was expressed as: $R'_{\text{total}} = R'_u + R'_b$, where the R'_u and R'_b were the values of the variable resistance units in the original state. Once a deformation of the AP sensor happened, the value of the variable resistance unit would be changed to make a response. The difference in resistance change was calculated as: $\Delta R_{\text{total}} = R''_{\text{total}} - R'_{\text{total}} = R''_u + R''_b - R'_u - R'_b$, where the R''_u and R''_b were the values of the variable resistance units in the stretched state. Therefore, it could be judged whether there was a deformation from the corresponding resistance of the AP sensor. Besides, further the deformation increased, the corresponding resistance of the AP sensor would continue to change. Through judging the change of the corresponding resistance, the AP sensor could be used to detect the size or degree of the deformation. In such a way, intelligent prostheses and soft robots embedded with the AP sensor could get the proprioception, whichever changing in joints would be confirmed by information from the AP sensor.

The stretchable active thread, which was the key functional composite material of the AE sensor and AP sensor, was composed of CNTs, polyester fibers, and rubber fiber (**Figure 2**a). A pure stretchable thread was the composite that two bundles of polyester fibers were alternately twisted with an elastic rubber fiber. By a pre-stretching coating method, CNTs were coated on

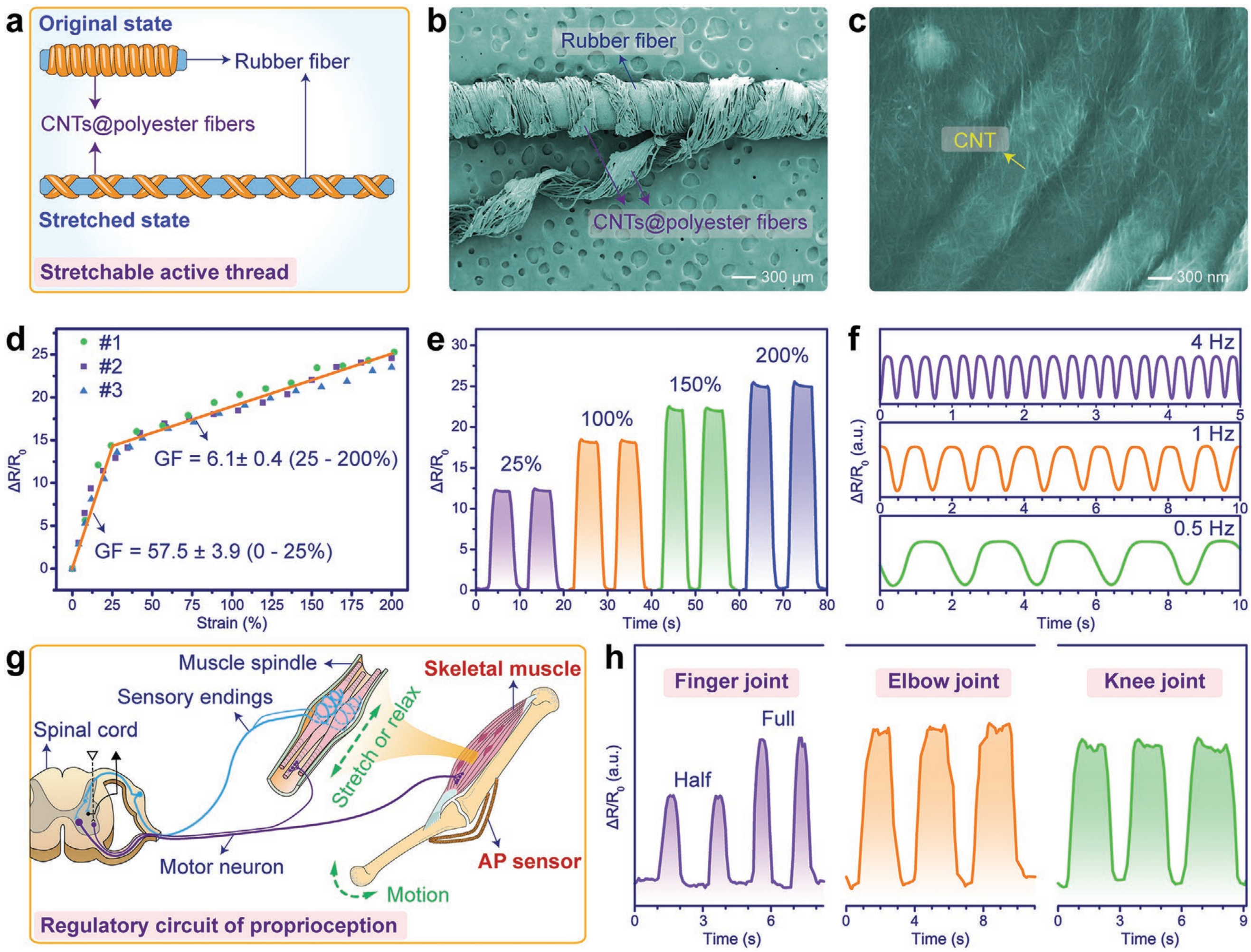

Figure 2. Stretchable active thread and performance of the AP sensor. a) Structure of the stretchable active thread. b) SEM image of the stretchable active thread where one bundle of polyester fibers coated with CNTs (CNTs@polyester fibers) peeled away the rubber fibers and the other bundle still twisted the rubber fiber. c) SEM image of the CNTs, which are coated on the polyester fibers. d) Relative change in resistance of the AP sensor under different strains, where showing the performance based on three identical devices. e) The tests on the response and recovery properties of the AP sensor by applying relatively large stretching strains. f) Normalized resistance response of the AP sensor under cyclically stretching loads (≈20% strain) with different frequencies. g) Regulatory circuit of proprioception, where the AP sensor is attached on the back side of movable joint. h) Bending activities of finger joint, elbow joint, and knee joint recorded by the AP sensor.

the pure stretchable thread. After this, the stretchable thread coated with CNTs (CNTs@stretchable thread) would be conductive and thus, could be served as the stretchable active thread (Figure S1, Supporting Information). Figure 2b shows the scanning electron microscope (SEM) image of the stretchable active thread, where one bundle of polyester fibers coated with CNTs (CNTs@polyester fibers) was peeled away the rubber fibers and the other bundle still twisted the rubber fiber. The SEM image of the CNTs that were coated on the polyester fibers was presented in Figure 2c. Movie S1, Supporting Information, vividly shows the high deformation of the stretchable active thread. In the movie, the black one was the bundle of CNTs@polyester fibers, which twisted the white line one that was the rubber fiber. It could be found that during stretching the stretchable active thread, the bundles of CNTs@polyester fibers always twisted the rubber fiber. The design method of the cross-scale heterogeneous structure of the stretchable active thread contributed to the as-fabricated devices to efficiently and steadily function.

As stated above, the AP sensor was based on the U-type configuration of the stretchable active thread. To reflect the electromechanical performance of the AP sensor, the relative change in resistance of the AP sensor was tested (Figure 2d). The relative change in resistance was calculated as: $\Delta R/R_0 = (R - R_0)/R_0$, where the R and R_0 were the values of the resistance of the AP sensor in the stretched state and the original state, respectively. The trend of the curve was to rise sharply first (0–25% strain), and then continued to rise relatively slowly (25–200% strain). There were two main factors that affected the change in resistance. One factor was the crack between the two bundles of the CNTs@polyester fibers and the other one was the contact area of the two bundles of the CNTs@polyester fibers (Figure S2, Supporting Information). Within the 25% strain, some cracks appeared with stretching. Then, their size began to expand and their number increased. The resistance changed rapidly at this stage. In the range of 25–200% strain, the number and size of cracks had a reduced ability to influence the resistance of the AP sensor, while the contact area of two bundles of the CNTs@polyester fibers became the main factor to affect the resistance. It should be noted that the change in contact area to affect the resistance was not as great as the effect of the change in the cracks. Therefore, at this stage, the resistance of the AP sensor continued to increase, but the change in the resistance was relatively slow compared to the one at the first stage. In this work, the GF, which was a parameter of sensitivity, of the AP sensor was defined as: $GF = \Delta R/R_0/\Delta\varepsilon$, where the $\Delta\varepsilon$ was the change in strain of the AP sensor being stretched. As shown in Figure 2d, the GF of the AP sensor ranged from 57.5 ± 3.9 (0–25% strain) to 6.1 ± 0.4 (in the large range of 25–200% strain). The high sensitivity of the AP sensor benefited a better detection within 25% strain, whose GF was over 28 times than that of metal-based sensors (GF ≈ 2). With an outstandingly large sensing range (0–200% strain) that was 40 times than that of metal-based sensors (≈5% strain), the AP sensor provided a powerful sensing platform to allow high integration of intelligent prostheses with the human body, and to efficiently adapt and monitor large deformation of soft robots.

Under static stretching strain, the tests on the response and recovery properties were conducted to probe the electromechanical stability of the AP sensor (Figure 2e). Several relatively large stretching strains of 25%, 100%, 150%, and 200% were applied on the AP sensor. The result showed that the AP sensor responded differently to the strains and the response was stable despite small overshoots generated by the delayed creep of the rubber fiber. Furthermore, the response frequency of the AP sensor was tested at the different stretching frequencies (Figure 2f). The stretching strain of ≈20% was applied on the AP sensor at the frequencies of 0.5, 1, and 4 Hz. These dynamic responses were continuous and stable. Damping and other significant changes in the dynamic responses did not happen from the AP sensor. The result manifested that the AP sensor possessed enough detection ability to accurately feedback the activities of various parts of the body within a normal frequency range. In addition, a microstrain (≈1%) was applied rapidly to evaluate the response time of AP sensor (Figure S3a, Supporting Information). The result showed the fast response time and decay time of the AP sensor were both <18 ms that was enough outstanding for normal operations in daily lives. The tests of more than 10 000 stretching-releasing strain cycles were conducted by applying 25% and 100% strains (Figure S3b, Supporting Information), which confirmed the satisfactory robustness and high stability of the AP sensor.

In the regulatory circuit of proprioception, skeletal muscle was connected at either or both ends to a bone and characterized by transverse stripes (Figure 2g). It provided muscle motor sensation, which mainly referred to the degree of muscle contraction and the change in the position of the extremities, and so moved parts of the skeleton. The muscle motor sensation is generally obtained by specialized biological receptors. Muscle spindle, a specialized biological receptor in the skeletal muscle, was the location in the muscle fiber, and each fiber was coiled with sensory endings, which was responsible for detecting changes in muscle length and tension. Effective detection would provide better information feedback to the body. Since the AP sensor featured high sensitivity, large sensing range, and fast and stable response, the different activities of various parts of the body would be accurately detected by equipping the corresponding parts with the AP sensor. As shown in Figure 2h, the dynamic curve from the AP sensor recorded the bending process of a finger. Different bending degrees of the finger, such as half bending and full bending, were distinctly measured and well recognized by the AP sensor. Besides, the motions of elbow joint and knee joint were also accurately reflected by the dynamic curves from the AP sensor. All the cyclical responses of the AP sensor were stable for the detection of these joints' bending motions. The results demonstrated that the AP sensor could yield significant information about the movement and position of the body and its parts. The AP sensor had the huge potential to supply the important perception foundation of proprioception for intelligent prostheses and soft robots.

The AE sensor could be also fabricated by the stretchable active threads based on the free conductive gate structure. As the parallel configuration of two stretchable active threads was adopted, the AE sensor featured high stretchability. In the original state, when an external mechanical stimulation was applied to the S_1 location of the AE sensor, the corresponding response resistance would be generated (**Figure 3**a). Since the response resistance of the AE sensor was linear with the location

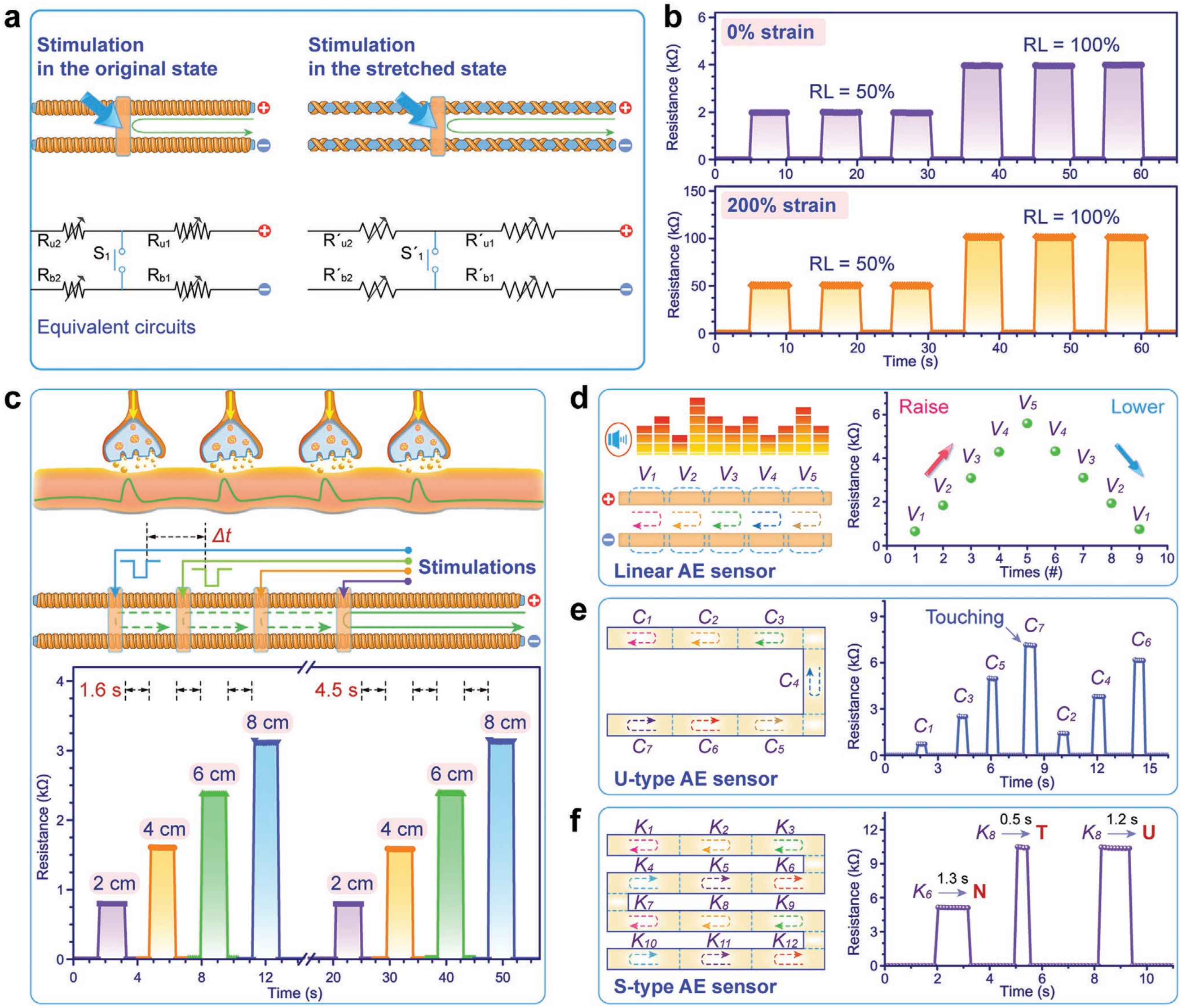

Figure 3. Performance and characteristics of the AE sensor. a) The working mechanism of the AE sensor in the original state and stretched state and their corresponding equivalent circuits. Longer effective working length by stretching the AE sensor brought more available portion to perceive the external mechanical stimulation. b) The change in the response resistance versus RL, where the external mechanical stimulation is applied on the original and stretched AE sensor, respectively. c) Spatiotemporally dynamic stimulations applying on the AE sensor. Top: Diagram of biological synapses and the AE sensor subjected to the external mechanical stimulation. Bottom: Repetitive responses to the dynamic stimulation applied on different location of the AE sensor at the interval time of 1.6 and 4.5 s, respectively. d) Music control demonstrated by using a linear AE sensor. e) A U-type AE sensor used for playing game and its typical resistance responses. f) Wireless typing based on an S-type AE sensor and its typical resistance responses.

(Figure S4a, Supporting Information), the relative location (RL) of the external mechanical stimulation would be confirmed by the formula: $RL = S_1/L = R_{S1}/R_L$, where the L was the length of the AE sensor, the R_{S1} and R_L were the response resistances of the AE sensor when the external mechanical stimulation was respectively applied on S_1 location and the end location. During deformation, the S_1 location and the length of the AE sensor were changed into S'_1 location and L'. Thus, once the external mechanical stimulation was applied to the S'_1 location, the RL of the AE sensor was the same as the one of the original AE sensor. As there was still a linear relationship between the response resistance and the location (Figure S4b, Supporting Information), the RL of the stretched AE sensor could be also calculated as: $RL = S'_1/L' = R'_{S1}/R'_L$, where the R'_{S1} and R'_L were the response resistances of the stretched AE sensor when the external mechanical stimulation was respectively applied on S'_1 location and the end location of the stretched AE sensor. As shown in Figure 3b, when the external mechanical stimulation was applied on the 50% RL, a response signal would be generated no matter whether the AE sensor was in a stretched state. Furthermore, a new different response signal from the AE sensor would occur once the RL of the external mechanical stimulation changed. The results manifested that the AE sensor had the ability to perceive external mechanical stimulation and could accurately recognize the location of the external mechanical stimulation. Even when being greatly stretched, the

AE sensor was still capable of stable functioning, which genuinely provided an essential exteroception to promote intelligent prostheses and soft robots into sophistication.

Biologically, dynamical stimulations at intervals can trigger synapses to induce neural signals and thus, form a spatiotemporally dynamic logic in a neural network (Figure 3c). In such a way, the brain would decide a feedback based on the neural signals. Since the AE sensor featured the highly regional differentiated response resistances to the location of external mechanical stimulation, a typical and basic spatiotemporally dynamic logic of the neural network could be mimicked by the AE sensor. For the demonstration, the AE sensor with length of 10 cm was fabricated. A short-term mechanical stimulation at the interval time of 1.6 s was successively applied on the locations of 2, 4, 6, and 8 cm, such that the mechanosensitive signal with different resistance was generated from the AE sensor. Furthermore, the long-term mechanical stimulation at the interval time of 4.5 s was also reflected well by the mechanosensitive signal of the AE sensor. Besides, the distinguishable and stable mechanosensitive signal could be generated to these dynamical stimulations even when greatly stretching the AE sensor, which indicated that the response of the AE sensor was highly robust (Figure S5, Supporting Information). The response from the AE sensor was analogous to the one of biological neural system, which was induced by different synapses from numerous mechanoreceptors. Note that the AE sensor did not need the integration of numerous sensing elements to respond to the spatiotemporally dynamic stimulations. It benefited to greatly simplify device's structure, reduce preparation process, and improve operating efficiency. For the use of the AE sensor, the response time and response stability were also important factors to be considered. As shown in Figure S6a, the AE sensor characterized a rapid response time and decay time of both <9 ms, providing a huge advantage for real-time feedback of signals. The tests of more than 10 000 loading–unloading cycles were conducted by applying the mechanical stimulation at different locations, which indicated the high stability and repeatability of the AE sensor (Figure S6b, Supporting Information).

Synaptic plasticity refers to the connection between neural cells, namely the synapse, whose connection strength can be adjusted.[28] Synapses will be strengthened and weakened as their activities changed. In our design, the AE sensor combined with logical operation could realize the functions of synaptic plasticity. To test the bionic synaptic plasticity, the AE sensor with length of 10 cm was prepared, in which two working portions were set (Figure S7a, Supporting Information). In this situation, the effective working length of each working portion was 5 cm, each of which was embedded with a couple of virtual mechanoreceptors and synapses. Through applying mechanical stimulation to the working portions multiple times, a database of the response signals would be obtained. Then, a rule of logical operation could be built to determine which working portion the unknown mechanical stimulation was applied on. After that, same feedback could be provided by applying the mechanical stimulation on the same working portion. It should be noted that the increase in times of mechanical stimulation would enrich the database, such that the rule of logical operation could be more reasonable and effective, which was like strengthening synapses in biology. In another aspect, more working potions with effective working length of 2 cm could be set in the AE sensor, so that more feedbacks could be provided to respond to more different locations of the mechanical stimulation (Figure S7b, Supporting Information). Based on the obtained database of the response signals, the rule of logical operation needed to be changed accordingly. In such a way, the new working potions could be obtained, which was like generating new connection between neural cells in biology. The characteristic of the bionic synaptic plasticity endowed the AE sensor with powerfully interactive capabilities, meaning that our thoughts could be precisely turned into scheduled actions by touching the corresponding working portion of the AE sensor.

As a proof of concept, there were five working portions in a linear AE sensor, to each of which the effective working length was 3 cm (Figure 3d and Figure S8a, Supporting Information). These five working portions, namely V_1, V_2, V_3, V_4, and V_5, corresponded to <20%, 20–40%, 40–60%, 60–80%, and >80% volume. Touching the corresponding working portion of the linear AE sensor could adjust the volume of music. Vivid music control by touching the linear AE sensor was shown in Movie S2, Supporting Information. Owing to the scalability of the preparation process, a U-type AE sensor with the seven working potions was designed (Figure 3e and Figure S8b, Supporting Information). These seven working potions were named C_1, C_2, C_3, C_4, C_5, C_6, and C_7. In a computer game, a gopher would randomly emerge from a hole. Touching a working portion of the U-type sensor would cause a virtual hammer to hit the gopher on the corresponding hole (Movie S3, Supporting Information). In addition, an S-type AE sensor with twelve working potions was also designed for wireless typing (Figure 3f and Figure S8c, Supporting Information). The working potions were named from K_1 to K_{12} in sequence. In a customized typing system, each virtual key included multiple characters. By touching a working portion of the S-type AE sensor, the characters inside the corresponding virtual key would start to display circularly. The display time of each character was 0.75 s. Once removing the touch, the character displayed at this time would be entered into the upper textbox and the key screen returned to its original state. Movie S4, Supporting Information, demonstrated that the text of "NTU SG!" was wirelessly typed by touching the S-type AE sensor. Through a reasonable path planning, only one as-designed fiber-shaped AE sensor could be used for touch perception on all sides around a three-dimensional hexagonal structure (Figure S9, Supporting Information). These demos manifested the powerfully interactive capabilities of the AE sensor and its superior performance. Multiple types of the AE sensor were successfully fabricated to indicate the superior universality of the design principle. It is thought-provoking to further consider additional demonstrations to emphasize the importance of the high stretchability of the devices. Nevertheless, we believe that, based on the highly stretchable devices, more exciting demos will be displayed in the future, and for example, future robots will be implemented as the Elastigirl in *The Incredibles*. It should be noted that as the CNTs dispersion was water-based, water would dissolve the CNTs of the dried CNTs@stretchable thread again if the devices were used in a humid or rain environment, which would lead to the devices failure. It needs further study to make the devices washable or waterproof to more close to real applications.

Like the sensory functions of receptors in the biological peripheral neural system, the integration of the AP sensor and AE sensor based on the stretchable active thread could provide the proprioception and exteroception of artificial peripheral neural system. The proposed artificial peripheral neural system had the great potential to promote prostheses and soft robots into being conscious. The schematic process flow of the artificial peripheral neural system based on the AP sensor and AE sensor included signal acquisition, central controller, neural network, and decision (**Figure 4**a). The joint activities could be detected by the AP sensor and the external mechanical stimulations were converted to digital signals by the AE sensor. The sensing circuit was implemented with an operational amplifier and a resistance to voltage conversion module (Figure 4b). The central controller module contained a low energy Bluetooth module (Taiyo Yuden EYSGCNZWY), which integrated a general-purpose system-on-chip (Nordic nRF51822) (Figure 4c). There were two main functions for this central controller: collecting and processing signals from the sensors and sending signals to back-end applications. When there was a resistance change on the sensor side introduced by external actions or deformations, a predefined command would be triggered and wirelessly delivered to back-end applications via a Bluetooth low energy (BLE) protocol. Since the front-end sensing circuit and the central controller module were integrated together on the same flexible board, the proposed system could be easily attached to human bodies with high comfortability. Through a logical operation, the features of the signals from the sensors were extracted. After that, the *k*-nearest neighbors algorithm was used to classify the joint activities and external mechanical stimulations. Based on the behavioral classification, an executable instruction would be triggered to feedback the decision, of which the potential applications included person identification, motion recognition, and wearable interaction.

Feature extraction was important to reduce the raw signal data to be informative and non-redundant. The typical sensory signal curves from the AP sensor and AE sensor were shown in Figure 4d. The deformation (D) of the AP sensor was set as a characteristic parameter for the joint bending within a set time of 5 s. Three characteristic parameters related to the signal curve of the AE sensor, including location of stimulation (L), holding time (H), and interval time (I), were set for the external mechanical stimulation within a set time of 9 s. As an example, when a finger bent two times within the set time, the AP sensor would detect the deformation of finger bending quickly. Subsequently, the deformation characteristic parameters were extracted by the self-defined logical operation. On the other hand, when an external mechanical stimulation, such as touch, was subsequently applied to the three different locations of the AE sensor, the activity of the external mechanical stimulation would be recorded in real-time within the set time. The corresponding characteristic parameters would also be extracted for further analysis and processing. All different activities of deformation and external mechanical stimulation could be characterized and classified by the feature map based on the four characteristic parameters (Figure 4e). The main idea of the classification was based on the *k*-nearest neighbors algorithm. For unknown activities detected from the AP sensor and AE sensor, their characteristic parameters would be compared to the database, which contained numerous characteristic parameters from the known activities. After that, the system could judge that the unknown activities were most likely to belong to which one that was known. Like the process of experience-dependent perceptual learning, the judgment could be more and more accurate by continuous learning and training, so that more appropriate feedback would be made for the interactive applications.

3. Conclusion

In summary, we proposed and demonstrated that two different types of AP sensor and AE sensor could be simultaneously fabricated by the novel functional composite of CNTs, polyester fibers, and rubber fiber through ingenious structural designs for artificial peripheral neural system. Attributed to the design method of cross-scale heterogeneous structure of the functional composite, both AP sensor and AE sensor featured outstandingly high stretchability that was unprecedented up to 200% stretching strain and exhibited the superior performance of fast response (<18 ms) and high stability (>10 000 cyclical tests), which ensured the efficient and stable operation of the artificial peripheral neural system. The artificial peripheral neural system based on the highly stretchable AP sensor and AE sensor was constructed and possessed both efficient exteroception and proprioception. Thereinto, the AE sensor realized the integrated functions, including detecting external stimulation, recognizing stimulation location, and transmitting mechanosensitive signal, and featured no energy consumption when no external stimulation occurred. The AP sensor characterized the high sensitivity and outstandingly wide sensing range, of which the GF was over 28 times and the sensing range was 40 times than that of metal-based sensors, respectively. Diverse joint activities of the body could be accurately detected by the AP sensor, and external mechanical stimulations could be effectively converted to digital signals by the AE sensor. It laid the extraordinary perception foundation of proprioception and exteroception for intelligent prostheses and soft robots with great elasticity. By combining with sensing circuit and logical operation, the artificial peripheral neural system performed extremely well and was as conscious and intelligent as humans and even beyond in certain aspects. Accurate feedback on the activities of various parts of the body, music control, game manipulation, and wireless typing manifested the enormous superiority of the spatiotemporal resolution function of the artificial peripheral neural system. This work not only provided a new and exciting way for simultaneously realizing two different types of highly stretchable bionic receptors but also constructed the high-performance artificial peripheral neural system, all of which would contribute to promoting intelligent prostheses and soft robots into sophistication, and would supply an alternative and highly powerful avenue for more convenient and fascinating lives in the future.

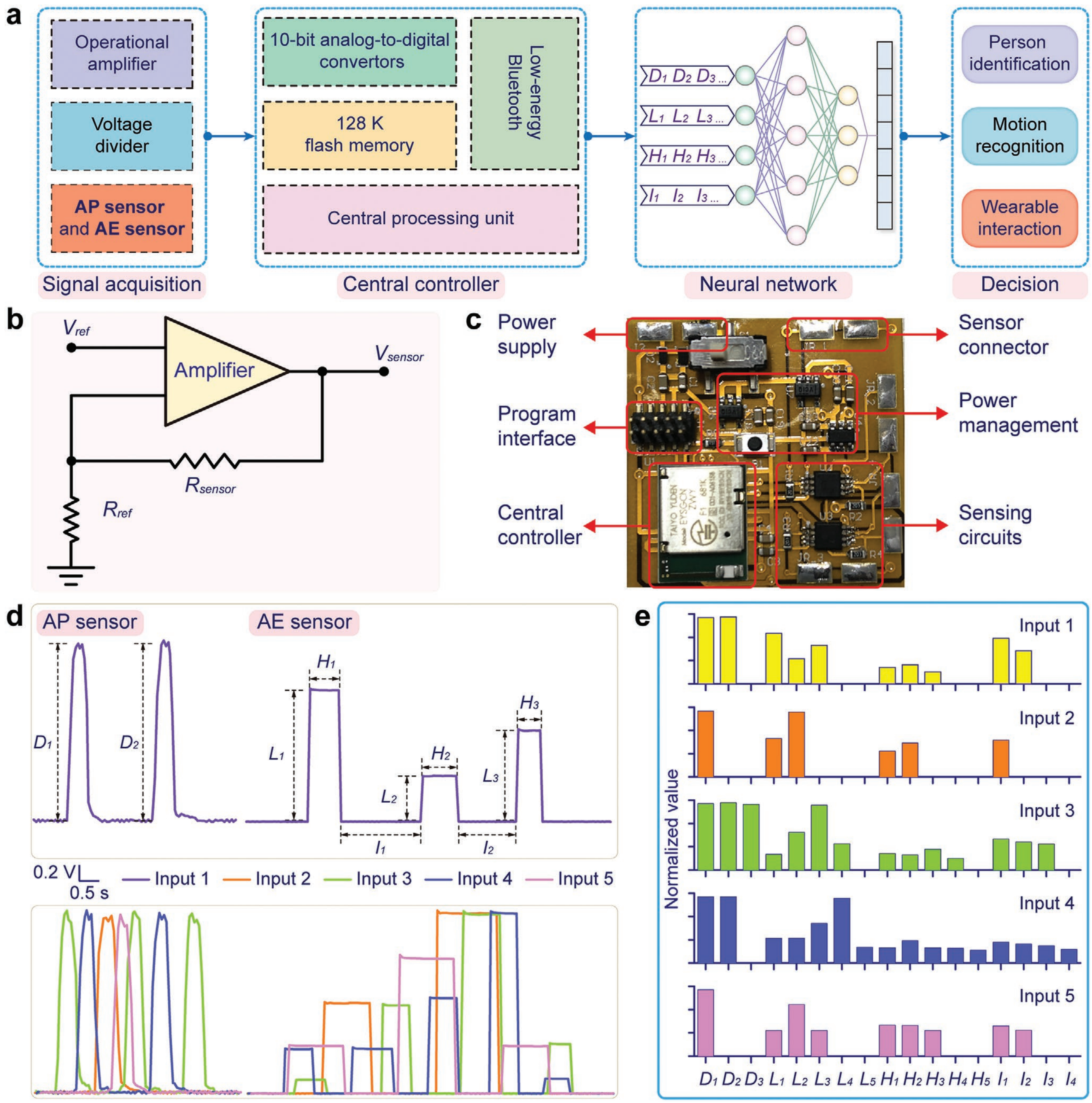

Figure 4. Coordination of the AP sensor and AE sensor. a) Schematic process flow of the artificial peripheral neural system based on the AP sensor and AE sensor, including signal acquisition, central controller, neural network, and decision. b) Circuit schematic to drive the AE sensor and AP sensor for applications. c) Main layout of the designed flexible PCB with the size of 3 × 3 cm^2. d) The typical sensory signal curves from the AP sensor and AE sensor, corresponding to different input information. The deformation (*D*) of the AP sensor is set as a characteristic parameter for the joint bending. Three characteristic parameters related to the signal curve of the AE sensor, including location of stimulation (*L*), holding time (*H*), and interval time (*I*), are set for the external mechanical stimulation. e) The feature map of the activities of deformation and external mechanical stimulation based on four characteristic parameters.

4. Experimental Section

Materials and Sensors Fabrication: A commercially available stretchable thread (22 YDS. PW22 ELASTIC THREAD, TONWEI, England) that two bundles of polyester fibers were alternately twisted with an elastic rubber fiber was selected as the basic elastic support. A pre-stretching coating method was used to coat the pure stretchable thread with CNTs. First, the pure stretchable thread was stretched and fixed in the ≈100% strain state by two binder clips, so that the bundles of polyester fibers would be separated. CNTs dispersion (water-based TNWDSR, Chengdu Organic Chemicals Co. Ltd.) was fully dip-coated on the pre-stretched pure stretchable thread by a dropper. Then, the wet stretchable thread was dried at room temperature for about 2 h. Five times of the coating–drying processes were performed to yield the CNTs@stretchable thread.

After that, the CNTs@stretchable thread was served as the stretchable active thread to fabricate the AP sensor and AE sensor. To fabricate the AP sensor, a U-type configuration of the stretchable active thread was adopted. In more details, a stretchable active thread was folded in half. Then, a pure stretchable thread was sandwiched between them to avoid contact between the folded parts of the stretchable active thread. The folding point of the stretchable active thread and the end of the pure stretchable thread were fixed together with a double-sided conductive copper foil tape (#1183, 3M Inc.). The two free ends of the stretchable active thread were respectively connected with a conductive wire. Their joints were fixed respectively with the double-sided conductive copper foil tape. Finally, the fixed joints and the other end of the pure stretchable thread were combined by an adhesive tape (Scotch Magic Tape 810, 3M Inc.). To fabricate the AE sensor, a parallel configuration of two stretchable active threads with the free conductive gate structure was adopted. Two stretchable active threads were placed in parallel and sandwiched a pure stretchable thread. The two ends of the stretchable active threads and the end of the pure stretchable thread on the same side were fixed together with the adhesive tape. The other ends of the stretchable active threads were respectively connected with a conductive wire. Their joints were fixed respectively with the double-sided conductive copper foil tape. Finally, the fixed joints and the other end of the pure stretchable thread were combined by the adhesive tape. The free conductive gate of the AE sensor was a double-sided conductive copper foil tape, which was attached to home-made loading equipment. Once an external mechanical stimulation was applied on the AE sensor by the loading equipment, the double-sided conductive copper foil tape would contact with the parallel stretchable active threads. For the demos of finger touching, the double-sided conductive copper foil tape was attached to a fingertip of a glove to serve as the free conductive gate. The photographs of the typical AP sensor and AE sensor were shown in Figure S10, Supporting Information.

Circuit Design and Signal Processing: The sensing circuit was implemented with an operational amplifier (Texas Instruments TLV2782) and resistance to voltage conversion module (Figure S9a, Supporting Information). The analog output voltage V_{sensor} from the sensing circuit had a linear relationship with the corresponding sensor resistance R_{sensor}. It could be expressed as: $V_{sensor} = V_{ref} \times (1 + R_{sensor}/R_{ref})$, where the V_{ref} and R_{ref} were the reference voltage and reference resistance. The operational amplifier provided 8 MHz bandwidth with only 650 µA of supply current, which made it dedicated for low-power and high-speed applications. The reference resistance and reference voltage were chosen as needed, making the analog output voltage within the analog to digital conversion input limitation of 3 V from the Bluetooth module. The central controller module was implemented by a low energy Bluetooth module (Taiyo Yuden EYSGCNZWY), which integrated a general-purpose system-on-chip (Nordic nRF51822) (Figure S9b, Supporting Information). There were 8 channels of 10-bit analog-to-digital convertor (ADC) integrated on this chip and four of them were configured to connect with the front-end sensing circuit on the flexible printed circuit board (PCB). The remaining ADCs were configured in their disabled mode so as to reduce total power consumption. Active ADC continuously monitored the sensor value at a sampling speed of 1000 times per second when there was a sensor connected to it. This Bluetooth module had an embedded 128 k programmable flash memory so that it could store the sensor data for a certain period depending on the sensing speed required for back-end applications. When there was a resistance change on the sensor side introduced by external actions or deformations, a predefined command would be triggered and wirelessly delivered to back-end applications via a BLE protocol. When compared to the classic Bluetooth technology, BLE featured less power consumption, which made it ideal for portable devices by providing longer battery life. Since the front-end sensing circuit and the central controller module were integrated together on the same flexible board, this proposed system could be easily attached to human bodies with high comfortability.

Characterization and Measurement: SEMs (FESEM 6340F and SEM JEOL 6360) were used to observe the morphologies of the materials. A digital optical microscope (UM012C, GAOSUO) was utilized to capture the dynamic process of stretching a stretchable active thread. Dynamic and static loading, including applying an external mechanical stimulation on the AE sensor and stretching the AP sensor, were performed by a customized actuator (Beijing Times Brilliant Electric Technology Co., Ltd.). The changes in resistance of the sensors were detected and recorded by digital multimeters (VICTOR 187 and Agilent 34461A). The current-voltage curves were measured by a semiconductor characterization system (Keithley 4200).

Supporting Information

Supporting Information is available from the Wiley Online Library or from the author.

Acknowledgements

This work was supported by the Program of Nanoantenna Spatial Light Modulators for Next Generation Display Technology (No. A18A7b0058), the grant from Guangdong Science and Technology Department (2020B1212060018), Singapore National Research Foundation's Returning Singapore Scientist Scheme (No. NRF-RSS2015-003), and AME programmatic funding scheme of Cyber Physiochemical Interface project (No. A18A1b0045).

Conflict of Interest

The authors declare no conflict of interest.

Data Availability Statement

Research data are not shared.

Keywords

bionic sensors, carbon nanotubes, fiber materials, functional composites, highly stretchable devices

Received: February 2, 2021
Revised: March 1, 2021
Published online:

[1] A. Damasio, G. B. Carvalho, *Nat. Rev. Neurosci.* **2013**, *14*, 143.
[2] L. Xu, W. Li, V. Voleti, D. J. Zou, E. M. C. Hillman, S. Firestein, *Science* **2020**, *368*, eaaz5390.
[3] J. Wu, A. H. Lewis, J. Grandl, *Trends Biochem. Sci.* **2017**, *42*, 57.
[4] S. J. Bensmaia, L. E. Miller, *Nat. Rev. Neurosci.* **2014**, *15*, 31.
[5] S. H. Woo, V. Lukacs, J. C. de Nooij, D. Zaytseva, C. R. Criddle, A. Francisco, T. M. Jessell, K. A. Wilkinson, A. Patapoutian, *Nat. Neurosci.* **2015**, *18*, 1756.
[6] S. Felton, M. Tolley, E. Demaine, D. Rus, R. Wood, *Science* **2014**, *345*, 644.
[7] M. Ortiz-Catalan, E. Mastinu, P. Sassu, O. Aszmann, R. Branemark, *N. Engl. J. Med.* **2020**, *382*, 1732.
[8] J. M. Hahne, M. A. Schweisfurth, M. Koppe, D. Farina, *Sci. Robot.* **2018**, *3*, eaat3630.
[9] S. I. Rich, R. J. Wood, C. Majidi, *Nat. Electron.* **2018**, *1*, 102.
[10] D. Rus, M. T. Tolley, *Nature* **2015**, *521*, 467.

[11] M. D. Lima, N. Li, M. Jung de Andrade, S. Fang, J. Oh, G. M. Spinks, M. E. Kozlov, C. S. Haines, D. Suh, J. Foroughi, S. J. Kim, Y. Chen, T. Ware, M. K. Shin, L. D. Machado, A. F. Fonseca, J. D. Madden, W. E. Voit, D. S. Galvao, R. H. Baughman, *Science* **2012**, *338*, 928.
[12] V. Mien, G. Shuzhi Sam, R. Hongliang, *IEEE Trans. Cybern.* **2017**, *47*, 1681.
[13] Y. Li, G. Carboni, F. Gonzalez, D. Campolo, E. Burdet, *Nat. Mach. Intell.* **2019**, *1*, 36.
[14] F. Suárez-Ruiz, X. Zhou, Q.-C. Pham, *Sci. Robot.* **2018**, *3*, eaat6385.
[15] H. K. Yap, P. M. Khin, T. H. Koh, Y. Sun, X. Liang, J. H. Lim, C.-H. Yeow, *IEEE Robot. Autom. Lett.* **2017**, *2*, 1383.
[16] Z. Chen, R. D. Kibler, A. Hunt, F. Busch, J. Pearl, M. Jia, Z. L. VanAernum, B. I. M. Wicky, G. Dods, H. Liao, M. S. Wilken, C. Ciarlo, S. Green, H. El-Samad, J. Stamatoyannopoulos, V. H. Wysocki, M. C. Jewett, S. E. Boyken, D. Baker, *Science* **2020**, *368*, 78.
[17] L. Mennel, J. Symonowicz, S. Wachter, D. K. Polyushkin, A. J. Molina-Mendoza, T. Mueller, *Nature* **2020**, *579*, 62.
[18] X. Liao, W. Song, X. Zhang, C. Yan, T. Li, H. Ren, C. Liu, Y. Wang, Y. Zheng, *Nat. Commun.* **2020**, *11*, 268.
[19] C. Liu, H. Chen, X. Hou, H. Zhang, J. Han, Y. G. Jiang, X. Zeng, D. W. Zhang, P. Zhou, *Nat. Nanotechnol.* **2019**, *14*, 662.
[20] X. Liao, W. Wang, M. Lin, M. Li, H. Wu, Y. Zheng, *Mater. Horiz.* **2018**, *5*, 920.
[21] X. Liao, W. Song, X. Zhang, H. Zhan, Y. Liu, Y. Wang, Y. Zheng, *Nano Energy* **2019**, *60*, 127.
[22] W. Wu, X. Wen, Z. L. Wang, *Science* **2013**, *340*, 952.
[23] T. Li, N. K. K. King, H. Ren, *IEEE Trans. Ind. Electron.* **2020**, *67*, 3236.
[24] X. Zhao, Z. Zhang, Q. Liao, X. Xun, F. Gao, L. Xu, Z. Kang, Y. Zhang, *Sci. Adv.* **2020**, *6*, eaba4294.
[25] X. Liao, Z. Zhang, Q. Liang, Q. Liao, Y. Zhang, *ACS Appl. Mater. Interfaces* **2017**, *9*, 4151.
[26] S. Chen, Y. Wei, S. Wei, Y. Lin, L. Liu, *ACS Appl. Mater. Interfaces* **2016**, *8*, 25563.
[27] S. R. Steinhubl, E. D. Muse, E. J. Topol, *Sci. Transl. Med.* **2015**, *7*, 283rv3.
[28] G. L. Collingridge, J. T. Isaac, Y. T. Wang, *Nat. Rev. Neurosci.* **2004**, *5*, 952.